

# LOCALIZED MICROMECHANICAL PROPERTIES OF FINE-PITCH SAC305 DOPED CARBON NANOTUBE SOLDER JOINTS

Norliza Ismail<sup>a</sup>, Muhammad Nubli Zulkifli<sup>b</sup>, A. Atiqah<sup>c\*</sup>

<sup>a</sup>Department of Applied Physics, Faculty of Science & Technology, Universiti Kebangsaan Malaysia (UKM), 43600 UKM Bangi, Selangor, Malaysia

<sup>b</sup>Electrical Engineering Section, Universiti Kuala Lumpur (UniKL), British Malaysian Institute (BMI), Batu 8, Jalan Sungai Pusu, 53100 Gombak, Selangor, Malaysia

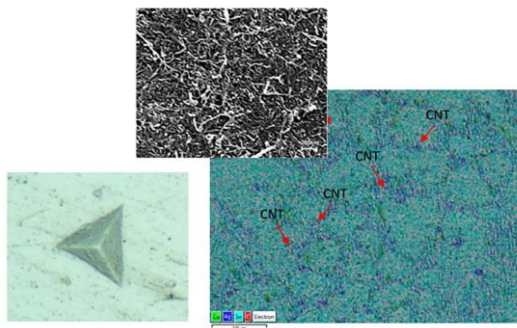
<sup>c</sup>Institute of Microengineering and Nanoelectronics (IMEN), Universiti Kebangsaan Malaysia, 43600 UKM Bangi, Selangor, Malaysia

## Article history

Received  
16 November 2021  
Received in revised form  
15 June 2022  
Accepted  
25 July 2022  
Published Online  
31 October 2022

\*Corresponding author  
a.atiqah@ukm.edu.my

## Graphical abstract



## Abstract

The addition of carbon nanotube (CNT) to the solder alloy has gained the attention due to its beneficially improve the mechanical properties of the solder alloy. Because of the miniaturization progress of electronic component, micromechanical properties of solder joint need to be focused instead of conventional mechanical properties. In this study, micromechanical properties, and deformation behaviour of SAC305 solder joints with the different CNT doping (weight percentage of 0.01, 0.02, 0.03 and 0.04) were investigated. Localized micromechanical properties included hardness, reduced modulus and stress exponent were determined via nanoindentation approach. Microstructural analysis was performed via optical microscope and field emission scanning microscope (FESEM). Doping of CNT in the SAC305 solder matrix changed the microstructure phase distribution. It was found that, doping of CNT, increase the near eutectic phase and decrease the primary  $\beta$ -Sn phase area. Furthermore, hardness values of SAC305 solder joint increased with increasing of CNT doping weight percentage. Hardness values of SAC305 solder joint increase about ~7 - 40% with the doping of CNT from 0.01 wt. % to 0.04 wt. %. However, localized reduced modulus and stress exponent show random values and no correlated trend with CNT doping were observed. Random values trend of stress exponent revealed that, SAC305 solder joint with the CNT doped involved the combination of deformation mechanism. This is due to the response of phase and CNT in the solder matrix to the localized indentation. In conclusion, a localized approach to hardness properties influenced by the CNT doping weight percentage. Contrary with the reduced modulus and stress exponent, which are not reliable on the CNT doping weight percentage.

**Keywords:** Lead free solder, carbon nanotube, nanoindentation, localized micromechanical properties, solder joint

## Abstrak

Penambahan karbon nanotub dalam aloi pateri telah menarik perhatian kerana bermanfaat dalam meningkatkan sifat mekanik aloi pateri. Disebabkan oleh perkembangan pengecilan komponen elektronik, sifat mikromekanik sambungan aloi pateri perlu difokuskan berbanding sifat mekanik konvensional. Dalam kajian ini, sifat mikromekanik dan tingkah laku ubah bentuk sambungan pateri SAC305 dengan pengedapan CNT yang berbeza (peratusan berat 0.01, 0.02, 0.03 dan 0.04) telah dikaji. Sifat mikromekanik setempat termasuk kekerasan, modulus terkurang dan eksponen tegasan ditentukan melalui pendekatan pelekukan nano. Analisis mikrostruktur dilakukan melalui mikroskop optik dan mikroskop pengimbasan pelepasan medan (FESEM). Pengedapan CNT dalam matriks pateri SAC305 telah mengubah taburan fasa mikrostruktur. Didapati bahawa, pengedapan CNT meningkatkan fasa hampir eutektik dan mengurangkan kawasan fasa  $\beta$ -Sn primer. Tambahan pula, nilai kekerasan sambungan pateri SAC305 meningkat dengan peningkatan peratusan berat pengedapan CNT. Nilai kekerasan sambungan pateri SAC305 meningkat kira-kira ~7 - 40% dengan pengedapan CNT daripada 0.01 wt. % hingga 0.04 wt. %. Walau bagaimanapun, modulus terkurang setempat dan eksponen tegasan menunjukkan nilai rawak dan tiada corak yang berkaitan dengan pengedapan CNT diperhatikan. Corak rawak nilai eksponen tegasan menunjukkan sambungan pateri SAC305 yang didopkan dengan CNT melibatkan gabungan mekanisma ubah bentuk. Ini disebabkan oleh tindak balas fasa dan CNT dalam matriks pateri terhadap pelekukan setempat. Kesimpulannya, pendekatan setempat terhadap sifat kekerasan dipengaruhi oleh peratusan berat pengedapan CNT. Bertentangan dengan modulus terkurang dan eksponen tegasan, yang tidak bergantung pada peratusan berat pengedapan CNT.

*Kata kunci:* Pateri bebas plumbum, karbon nanotub, pelekukan nano, sifat mikromekanik setempat, sambungan pateri

© 2022 Penerbit UTM Press. All rights reserved

## 1.0 INTRODUCTION

Lead free solder alloy is still widely used as the interconnection means for the electronic devices. This is due to its maturity and flexibility of usage in the manufacturing process [1–3]. Electronic products have wide range of applications and nowadays, higher performance in terms of robustness and electrical properties are critically demanded in the consumer product [4,5]. Thus, it has urged to the introduction of new type of solder alloys that can cater for the higher performance of robustness and electrical properties of electronic products. The reliability of soldered joint in electronic packaging depends on mechanical integrity. Occurrences of mechanical failure can cause electrical failure [6]. Mechanical integrity in turn, depends on mechanical properties. The mechanical properties of solder alloys are extremely important because solder joints must retain their mechanical integrity under a numerous of conditions such as creep, thermal fatigue, and mechanical shock and drop resistance [7].

Composite type of solder alloys has been widely introduced as one of the approaches to increase the mechanical properties of solder joints [8,9]. Carbon nanotube (CNT) is one of the discrete secondary particles that has been used to form composite solder

alloys. This is because CNT has exceptional mechanical properties and by mixing the CNT with solder alloy, some mechanical properties of that composite solder alloy could be improved. Several researchers have conducted to evaluate the mechanical properties of CNT doped solder alloys or joints composite. Kumar *et al.*, (2008) reported that the doping of CNT into Sn-Ag-Cu lead free solder has reduced the secondary phase of solder that lead to the increase of the hardness [10]. They also reported that the melting temperature of CNT-based composite solder was slightly reduced due the high surface energy and interfacial instability created with the doping of CNT into lead free solder. Niranjani *et al.*, (2011) observed that the addition of CNT into Sn-Ag-Cu lead free solder has increased the tensile properties of the solder [11]. They noted that the addition of 0.05 wt.% CNT to SAC387 lead free solder alloy has increased yield and ultimate tensile strength at varied temperatures and strain changes. Zhu *et al.*, (2018) doped into SAC307 solder joints with three different diameter of CNT and found that the moderate diameter of 40-60 nm has performed better in mechanical strength compared to that of either larger or smaller CNT [12]. Ismail *et al.*, (2022) that addition of CNT into Sn-Ag-Cu solder improve the mechanical properties of solder joint [13]. Besides, the existence of

CNT in the Sn-Ag-Cu solder system also increases the resistance of solder joint when expose to the blast wave.

Micromechanical properties of SAC doped CNT solder joints composite still requires further analysis to determine a more comprehensive data. Noticeably, many researchers have been studied the mechanical properties on the bulk solder form rather than on solder joint form [14-16]. In the application, solder joint involves the chemical reaction of the solder and the substrate, which is opposite to the solder bulk condition. Therefore, it is vital to evaluate the micromechanical properties of solder joint as compared to solder bulk to get the accurate properties. Nanoindentation become the valuable approach to determine the micromechanical properties of solder joint due to its localized measurement which is suit the down scale of solder joint. Nanoindentation provides viable and fast method to study the deformation behaviour of materials via creep data compared to conventional methods such as tensile test and compression test [17, 18]. Investigation on microstructure and localized micromechanical properties such as hardness, reduced modulus and stress exponent of SAC305 doped by variation composition of CNT were reported in this paper.

## 2.0 METHODOLOGY

Multiwalled carbon nanotube (CNT) nanoparticles with 10-20 nm diameter (Figure 1) were used as a dopant to the Sn-3.0Ag-0.5Cu (SAC305) solder paste system. SAC305 doped CNT solder paste were prepared by mechanically mixed the CNT nanoparticles that have different weight percentage (wt.%) of 0.01 wt.%, 0.02 wt.%, 0.03 wt.% and 0.04 wt.% with SAC305 solder powder and flux using vacuum mixer.

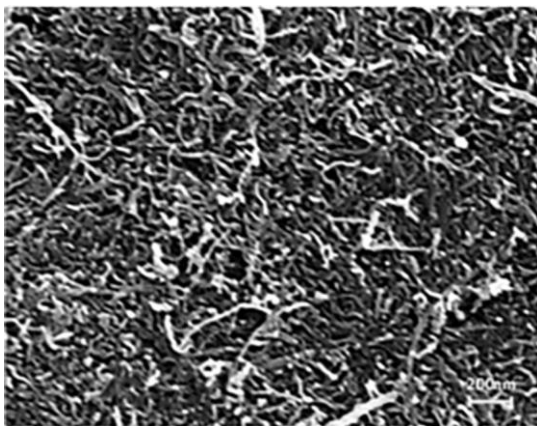


Figure 1 FESEM image of CNT raw material

Figure 2 show the FESEM image of SAC305 doped CNT solder paste. SAC305 doped CNT solder paste

were soldered on the copper, Cu pads with size of  $(0.33 \times 0.33)$  mm<sup>2</sup> on the printed circuit board (PCB) using infrared (IR) reflow based on the J-STD-020D JEDEC standard to create fine-pitch SAC305 doped CNT solder joints [19]. Figure 3 shows the location of fine pitch of SAC305 solder joints.

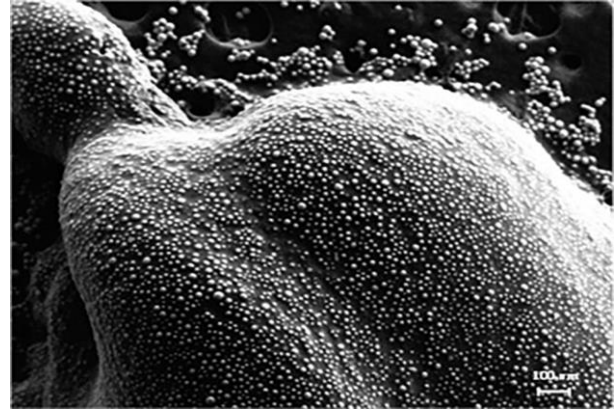


Figure 2 FESEM image of SAC305 doped CNT solder paste

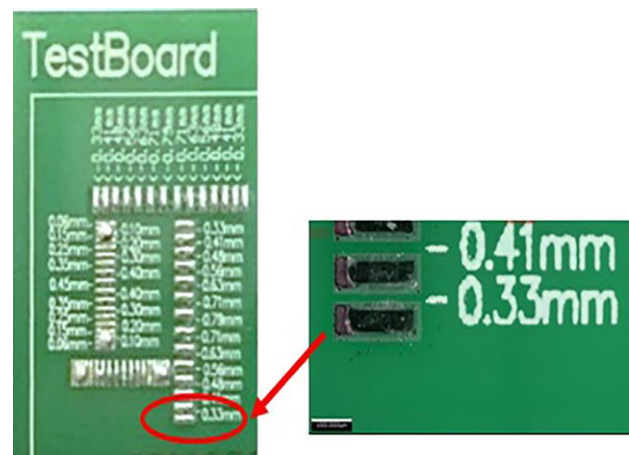


Figure 3 Location of fine-pitch SAC305 solder joints

Sample preparation for microstructure examination and nanoindentation test of SAC305 doped CNT solder joints were carried out using metallography technique. Firstly, cut samples were mounted using the resin. After the samples were cured, wet grinding was carried out with 600, 800, 1200 and 2000 grits of abrasive papers followed by polishing with 1 μm and 0.25 μm diamond suspensions on silk cloth. The samples were immersed into an etchant solution of 5% hydrochloric acid (HCL) and 95% methanol for 10 s then rinsed with deionized (DI) water. Microstructure examination of cross sectioned of SAC305 doped CNT solder joints were performed using Raxvision MM10A high power metallurgical microscope. The obtained optical micrograph images of the SAC305 doped CNT solder joints were further analysed using ImageJ processing software of ImageJ to determine the microstructural evolution due to CNT doping. Representative SAC305-CNT sample was characterize

using field emission scanning electron microscope (FESEM) Carl Zeiss brand Model Gemini SEM 500 to determine the existence of CNT in the solder matrix.

Nanoindentation test was carried out using a Micro Materials Nanotest™ nanoindentation machine equipped with a Berkovich diamond tip. Three indentations with 10 mN of load were indented on each sample with spacing of 12 μm as shown in Figure 4. Summary of experimental procedure was indicated in Figure 5. Nanoindentation test was performed at room temperature with loading and unloading rates of 0.5 mNs<sup>-1</sup>, 30 s hold time at the peak (dwell time) and 30 s hold time at 90 % unloading for thermal drift correction. Oliver and Pharr method were applied to measure the nanoindentation micromechanical data of hardness and reduced modulus [20].



Figure 4 Location of indentations on the SAC305 solder joints

Stress exponent which reflected to the deformation behaviour of SAC305 doped CNT solder joints was determined using the constant load method due to its popularity and maturity [21, 22]. To further analyse the deformation mechanism that could occurred during nanoindentation test on SAC305 doped CNT solder joints, the log-log graph of strain rate versus stress is plotted using the following equations:

$$\sigma = \frac{F}{A_p} \tag{1}$$

$$\dot{\epsilon} = \frac{1}{h} \frac{dh}{dt} \tag{2}$$

where  $\sigma$  is stress, F is applied load,  $A_p$  is indentation projected area, h is depth dh is depth gradient and dt is time gradient.  $A_p$  for Berkovich indenter is  $24.5 h^2$ .

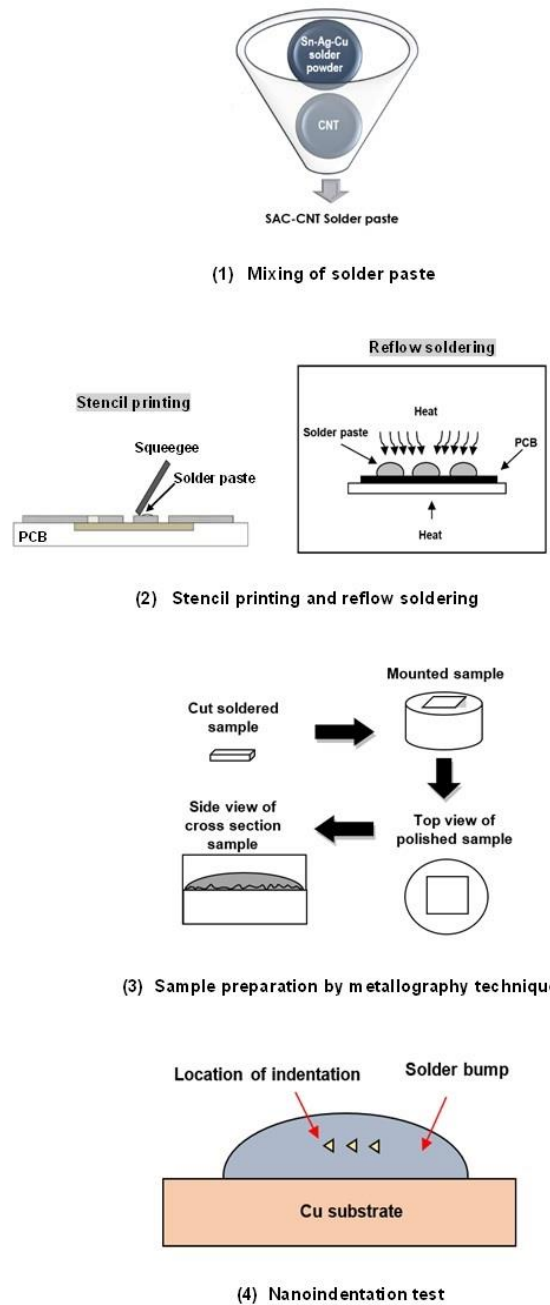
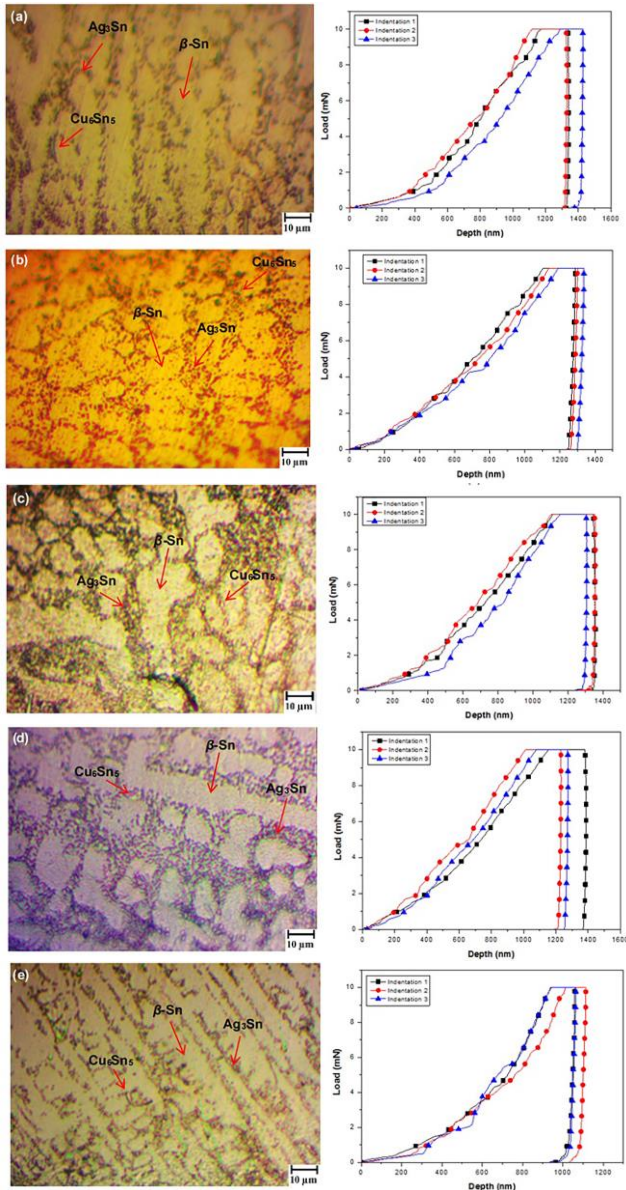


Figure 5 Summary of experimental procedure (drawing not to scale)

### 3.0 RESULTS AND DISCUSSION

Figure 6 shows the micrograph images of the SAC305 doped CNT solder joints with CNT weight percentage of 0 wt.% (SAC305), 0.01 wt.% (SAC305-CNT1), 0.02 wt.% (SAC305-CNT2), 0.03 wt.% (SAC305-CNT3) and 0.04 wt.% (SAC305-CNT4). Microstructure of SAC305 and SAC305 doped CNT generally contain the primary  $\beta$ -Sn phase, near eutectic region ( $\beta$ -Sn and  $Ag_3Sn$ ) and intermetallic compound  $Cu_6Sn_5$  [23]. CNT doping in the solder matrix was known is not react with the solder

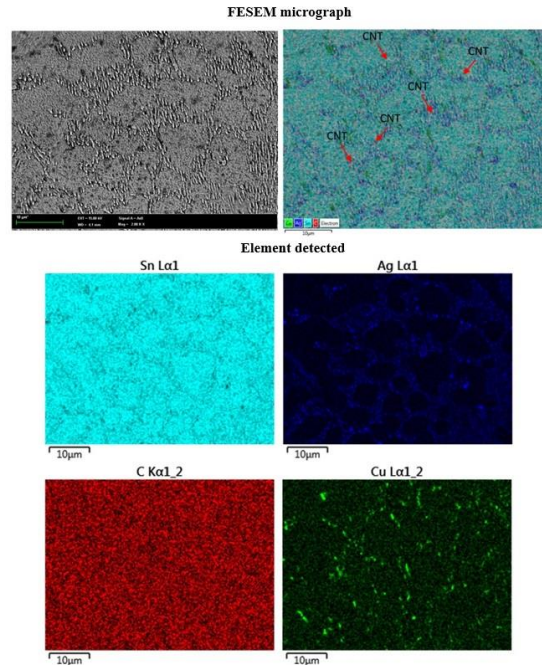
elements. Therefore, there is no additional phase form in the microstructure of SAC305 solder joint [24].



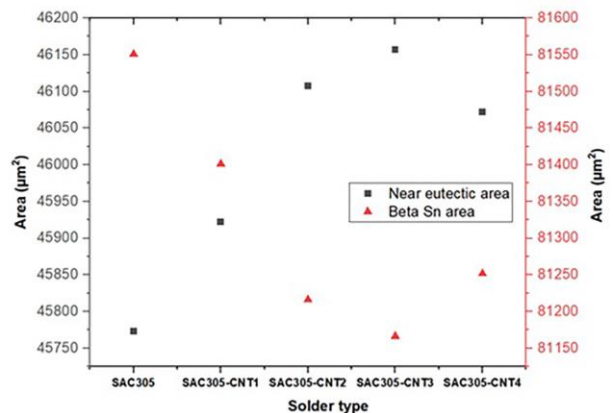
**Figure 6** Micrograph of SAC305 doped CNT solder joints with CNT weight percentage of a) 0 wt.%, b) 0.01 wt.%, c) 0.02 wt.%, d) 0.03 wt.% and e) 0.04 wt.% attached with the nanoindentation loading-unloading profiles

Figure 7 shows the representative FESEM micrograph of SAC-CNT solder. Existence of CNT in the solder matrix can be observed by the detection of carbon elements in the solder matrix. CNT tends to allocate near the eutectic region as similar with the observation done by Kumar et. al [10]. Measurement of area fraction performed by using ImageJ analysis revealed that the area of near eutectic increases with the addition of CNT up to 0.03 wt.% and slightly decrease at 0.04 wt.% of CNT as shown in Figure 8. Meanwhile, the  $\beta$ -Sn primary phase area trend is decrease with the addition of CNT up to 0.03 wt.% and

slightly increase at 0.04 wt.%. Three indentations randomly perform in solder matrix from different location (as shown in Figure 4) resulted to the variation of  $P$ - $h$  profiles respectively. Variations of  $P$ - $h$  profiles are due to the different phase existence in the solder matrix. It was known that  $\beta$ -Sn phase has a soft property compared to the near eutectic phase which also contain  $Ag_3Sn$  [25]. However, based on the indentation sizes, each of the indents were found to cover both phases included  $\beta$ -Sn and near eutectic phases. Thus, obtained  $P$ - $h$  profiles are in almost similar and acceptable range.



**Figure 7** Representative FESEM micrograph and EDS analysis of SAC305-CNT solder joint



**Figure 8** Variation of near eutectic and  $\beta$ -Sn primary phase area of SAC305 and SAC305 doped CNT solder joints

Figure 9 illustrates the variation of hardness versus SAC305 doped CNT solder joints. Hardness value is one of the quantitative micromechanical properties obtained from nanoindentation test. Hardness

properties of indented solder joint depend on the resistance of the material to the applied load towards deformation [26]. From Figure 8 it is noted that the hardness value increased with the increment of the CNT weight percentage. Existence of CNT in the solder matrix induced the high resistance to the deformation. CNT act as barrier to the applied load [27]. Although the measurements of the hardness properties are localized, the obtained values follow the trend of CNT addition weight percent. This is due to the indentation size covered both phase area which is near eutectic and  $\beta$ -Sn primary phase. This finding agrees with the other studies, reported that the addition of CNT have a significant effect towards increasing the hardness of solder alloys [28, 29, 30].

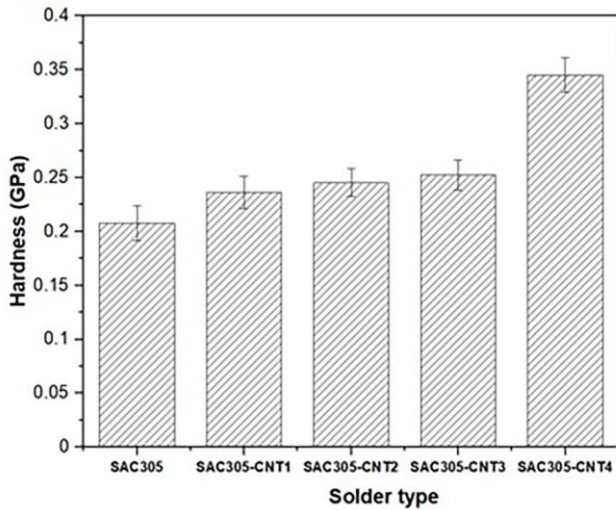


Figure 9 Variation of hardness towards the SAC305 doped CNT solder joints

Table 1 Hardness of SAC solders by CNT addition and other nanoparticles

Types solder	of	Types of Nanopar ticles	Types of Form	Test approach	Hardness (GPa)	Ref.
SAC305					0.207	
SAC305-CNT1		Carbon nanotub e (CNT)	Solder joint	Berkovich Nanoinde ntation	0.236	Current work
SAC305-CNT2					0.245	
SAC305-CNT3					0.252	
SAC305-CNT4					0.345	
SAC357		Carbon nanotub e (CNT)	Solder bulk	Vickers Microhard ness	0.159	[31]
SAC357-CNT1					0.163	
SAC357-CNT4					0.166	
SAC387		Silicon carbide (SiC)	Solder bulk	Vickers Microhard ness	0.158	[32]
SAC387-0.01SiC					0.206	
SAC387-0.05SiC					0.229	
SAC357-0.20SiC					0.207	

Types solder	of	Types of Nanopar ticles	Types of Form	Test approach	Hardness (GPa)	Ref.
SAC305		Cerium oxide (CeO <sub>2</sub> )	Solder joint	Vickers Microhard ness	0.1628	[33]
SAC305-1CeO <sub>2</sub>					0.1824	

Figure 10 shows the reduced modulus of SAC305 and SAC305 doped CNT solder joint. From the graph, doping of CNT decrease the reduced modulus values. However, obtained reduced modulus does not follow the CNT doping trend as indicated in hardness properties. Random values of reduced modulus can be observed in Figure 10 which is at 0.01 wt. %, the reduced modulus decrease before increase until up to 0.03 wt. % and slightly decrease at 0.04 wt. %. Contrast to the hardness properties which is represent the surface properties of materials, reduced modulus represents the intrinsic properties of the indented materials. Reduced modulus indicates the bond strength of the atoms of the materials [34]. The higher reduced modulus of the materials, the stiffer of the materials. Reduced modulus properties of SAC305 doped CNT obtained in this study remarkably opposite with other findings due to localized and sample form [28, 35].

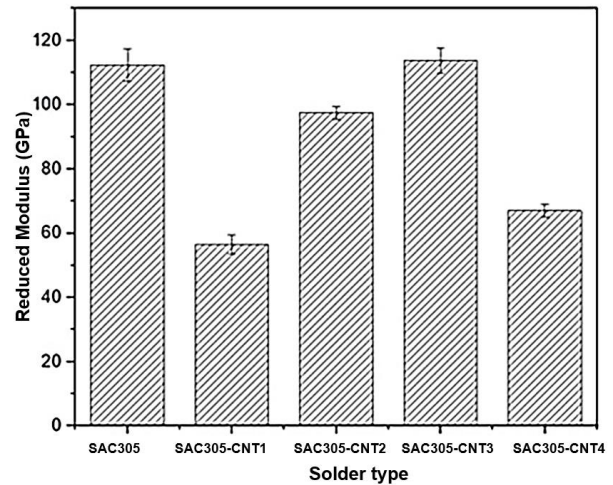
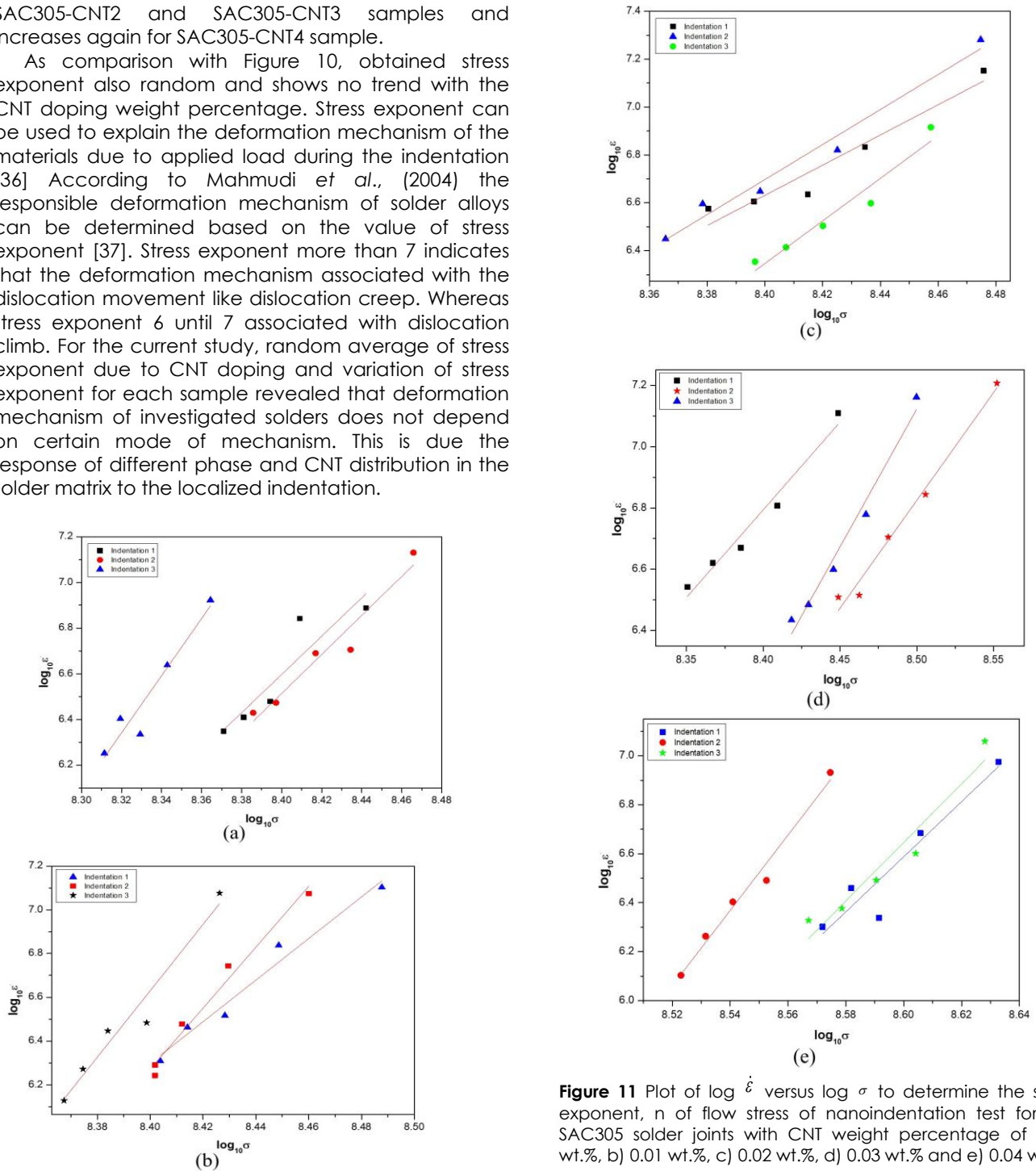


Figure 10 Variation of reduced modulus SAC305 doped CNT solder joints

Figure 11 indicates the plot of  $\log \dot{\epsilon}$  versus  $\log \sigma$  to determine the stress exponent, n of flow stress of nanoindentation test for the SAC305 and SAC305 doped CNT solder joints. the log-log graph of strain rate versus stress is plotted using the equations as stated in experimental procedures. From the plotted graphs, there are variation for each indentation of each sample due to localized indentations. In Figure 12 it is noted that the average stress exponent value increases from SAC305 to SAC305-CNT1 solder joints. Then the average stress exponent is reduced for both

SAC305-CNT2 and SAC305-CNT3 samples and increases again for SAC305-CNT4 sample.

As comparison with Figure 10, obtained stress exponent also random and shows no trend with the CNT doping weight percentage. Stress exponent can be used to explain the deformation mechanism of the materials due to applied load during the indentation [36]. According to Mahmudi *et al.*, (2004) the responsible deformation mechanism of solder alloys can be determined based on the value of stress exponent [37]. Stress exponent more than 7 indicates that the deformation mechanism associated with the dislocation movement like dislocation creep. Whereas stress exponent 6 until 7 associated with dislocation climb. For the current study, random average of stress exponent due to CNT doping and variation of stress exponent for each sample revealed that deformation mechanism of investigated solders does not depend on certain mode of mechanism. This is due the response of different phase and CNT distribution in the solder matrix to the localized indentation.



**Figure 11** Plot of  $\log \dot{\epsilon}$  versus  $\log \sigma$  to determine the stress exponent,  $n$  of flow stress of nanoindentation test for the SAC305 solder joints with CNT weight percentage of a) 0 wt.%, b) 0.01 wt.%, c) 0.02 wt.%, d) 0.03 wt.% and e) 0.04 wt.%

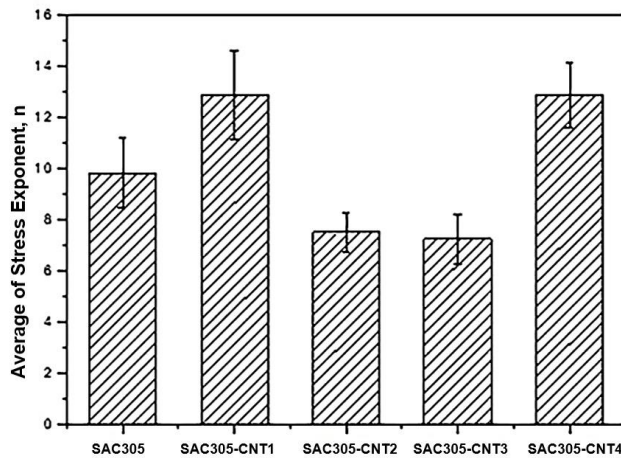


**Figure 12** Variation of stress exponent of flow stress towards SAC305 doped CNT solder joints

#### 4.0 CONCLUSION

This work was concentrated to access the localized micromechanical properties and deformation behaviour of SAC305 solder doped CNT with the variation of weight percentage (0.01 up to 0.04). This was performed by investigating the micromechanical properties included hardness, reduced modulus, and stress exponent by nanoindentation approach. Doping of CNT changed the microstructure phase distribution. The doping of CNT increases the near eutectic phase area and reduce the primary  $\beta$ -Sn phase area. Localized hardness properties were proportional to the amount of CNT doping. Hardness increases by about ~7% to 40% with CNT doping. Nevertheless, the localized approach by nanoindentation indicates that reduced modulus and stress exponent are random and have no trend with the amount of CNT doping. From the stress exponent results, it was concluded that the deformation mechanism participating in SAC305-CNT solder joint is combination mode and does not rely on one mode only due to the localized indentation. Since the nanoindentation has limitations, future work will focus on analysing the microstructure using transmission electron microscope (TEM) and electron back scattering diffraction (EBSD) to understand and obtain an image of how the mechanism occur at atomic scale.

#### Acknowledgement

The authors would like to acknowledge GGPM-2020-036 grant under Universiti Kebangsaan Malaysia for provide the funding of this research.

#### References

[1] McDougall, J., Choi, S., Bieler, T., Subramanian, and K., Lucas, J. 2000. Quantification of Creep Strain Distribution in

Small Crept Lead-Free In-Situ Composite and Non Composite Solder Joints. *Mater. Sci. Eng. A*. 285: 25-34. DOI: [https://doi.org/10.1016/S0921-5093\(00\)00661-4](https://doi.org/10.1016/S0921-5093(00)00661-4).

[2] Korhonen, T. M. K., Turpeinen, P., Lehman, L. P., Bowman, B., Thiel, G. H., Parkes, R. C., Korhonen, M. A., Henderson, D. W., and Pufflitz, K. J. 2004. Mechanical Properties of Near-eutectic Sn-Ag-Cu Alloy Over a Wide Range of Temperatures and Strain Rates. *J. Electron. Mater.* 33: 1581-1588. DOI: <https://doi.org/10.1007/s11664-004-0101-2>.

[3] El-Daly, A. A., and Hammad A. E. 2011. Development of High Strength Sn-0.7Cu Solders with the Addition of Small Amount of Ag and In. *J. Alloys Compd.* 509: 8554-8560. DOI: <https://doi.org/10.1016/j.jallcom.2011.05.119>.

[4] Che, F. X., and Pang, J. H. L. 2015. Study on Reliability of PQFP Assembly with Lead Free Solder Joints under Random Vibration Test. *Microelectron. Reliab.* 55: 2769-2776. DOI: <https://doi.org/10.1016/j.microrel.2015.09.010>.

[5] Khatibi, G., Betzwar Kotas, A., and Lederer, M. 2018. Effect of Aging on Mechanical Properties of High Temperature Pb-rich Solder Joints. *Microelectron. Reliab.* 85: 1-11. DOI: <https://doi.org/10.1016/j.microrel.2018.03.009>.

[6] Cheng, S., Huang, C. M., and Pecht, M. 2017. A Review of Lead-free Solders for Electronics Applications. *Microelectronics Reliability*. 75: 77-95. DOI: <https://doi.org/10.1016/j.microrel.2017.06.016>.

[7] Sona, M., and Prabhu, K. N. 2014. The Effect of Reflow Time on Reactive Wetting, Evolution of Interfacial IMCs and shear Strength of Eutectic Sn-Cu Solder Alloy. *Journal of Materials Science: Materials in Electronics*. 25(3): 1446-1455. DOI: <https://doi.org/10.1007/s10854-014-1749-x>.

[8] Sharma, A., Srivastava, A. K., Lee, K., and Ahn, B. 2019. Impact of Non-Reactive Ceria Nanoparticles on the Wettability and Reaction Kinetics between Lead-Free Sn-58Bi and Cu Pad. *Met. Mater. Int.* 25(8). DOI: <https://doi.org/10.1007/s12540-019-00250-1>.

[9] Nai, S. M. L., Gupta, M., Wei, J., Nai, J., Gupta, S. M. L., and Wei, M. 2008. Suppressing Intermetallic Compound Growth in SnAgCu Solder Joints with Addition of Carbon Nanotubes. *2nd IEEE Int. Nanoelectron. Conf. INEC 2008*. 15-19. DOI: <https://doi.org/10.1109/INEC.2008.4585428>.

[10] Kumar, K. M., Kripesh, V., and Tay, A. a. O. 2008. Single-wall Carbon Nanotube (SWCNT) Functionalized Sn-Ag-Cu Lead-free Composite Solders. *J. Alloys Compd.* 450: 229-237. DOI: <https://doi.org/10.1016/j.jallcom.2006.10.123>.

[11] Niranjani, V. L., Rao, B. S. S. C., Singh, V., and Kamat, S. V. 2011. Influence of Temperature and Strain Rate on Tensile Properties of Single Walled Carbon Nanotubes Reinforced Sn-Ag-Cu Lead Free Solder Alloy Composites. *Mater. Sci. Eng. A*. 529: 257-264. DOI: <https://doi.org/10.1016/j.msea.2011.09.026>.

[12] Zhu, Z., Chan, Y. C., Chen, Z., Gan, C. L., and Wu, F. 2018. Effect of the Size of Carbon Nanotubes (CNTs) on the Microstructure and Mechanical Strength of CNTs-doped Composite Sn0.3Ag0.7Cu-CNTs Solder. *Mater. Sci. Eng. A*. 727: 160-169. DOI: <https://doi.org/10.1016/j.msea.2018.05.002>.

[13] Wan Yusoff, W. Y., Ismail, N., Mohamad Lehan, N. F. N., Amat, A., Ku Ahmad, K. Z., Jalar, A. and Abdul Rahman, I. 2022. Micromechanical Response of SAC305 Solder Alloy under Gamma Radiation via Nanoindentation Approach. *Soldering & Surface Mount Technology*. Vol. ahead-of-print No. ahead-of-print. DOI: <https://doi.org/10.1108/SSMT-09-2021-0060>.

[14] Yang, L., Liu, H., Zhang, Y., & Yu, H. 2017. Study on the Reliability of Carbon Nanotube-Reinforced Sn-58Bi Lead-Free Solder Joints. *Journal of Materials Engineering and Performance*. 26: 12. DOI: <https://doi.org/10.1007/s11665-017-3033-8>.

[15] Yang, Z., Zhou, W., & Wu, P. 2014. Effects of Ni-coated Carbon Nanotubes Addition on the Microstructure and Mechanical Properties of Sn-Ag-Cu Solder Alloys. *Materials Science and Engineering A*. 590: 295-300. DOI: <https://doi.org/10.1016/j.msea.2013.10.008>.

- [16] Han, Y. D., Jing, H. Y., Nai, S. M. L., Xu, L. Y., Tan, C. M., & Wei, J. 2012. Interfacial Reaction and Shear Strength of Ni-coated Carbon Nanotubes Reinforced Sn-Ag-Cu Solder Joints during Thermal Cycling. *Intermetallics*. 31: 72-78. DOI: <https://doi.org/10.1016/j.intermet.2012.06.002>.
- [17] Jalar, A., Bakar, M. A., and Ismail, R. 2020. Temperature Dependence of Elastic-Plastic Properties of Fine-Pitch SAC 0307 Solder Joint Using Nanoindentation Approach. *Metallurgical and Materials Transactions A: Physical Metallurgy and Materials Science*. 51: 1221-1228. DOI: <https://doi.org/10.1007/s11661-019-05614-1>.
- [18] Ernst, B., Keim, S., and Tetzlaff, U. 2022. On the Anisotropic Indentation Modulus and Anisotropic Creep Behavior of  $\beta$ -Sn Characterized by Nanoindentation Methods. *Materials Science and Engineering: A*. 848: 143392. DOI: <https://doi.org/10.1016/j.msea.2022.143392>.
- [19] Bath, J. 2007. *Lead-Free Soldering Standards*, in: *Lead-Free Solder*. Springer US, Boston, MA. 271-284. DOI: [https://doi.org/10.1007/978-0-387-68422-2\\_10](https://doi.org/10.1007/978-0-387-68422-2_10).
- [20] Oliver, W. C., and Pharr, G. M. 2011. An Improved Technique for Determining Hardness and Elastic Modulus Using Load and Displacement Sensing Indentation Experiments. *J. Mater. Res.* 7: 1564-1583. DOI: <https://doi.org/10.1557/JMR.1992.1564>.
- [21] Goodall, R., and Clyne, T.W. 2006. A Critical Appraisal of the Extraction of Creep Parameters from Nanoindentation Data Obtained at Room Temperature. *Acta Mater.* 54: 5489-5499. DOI: <https://doi.org/10.1016/j.actamat.2006.07.020>.
- [22] Marques, V. M. F., Wunderle, B., Johnston, C., and Grant, P.S. 2013. Nanomechanical Characterization of Sn – Ag – Cu / Cu joints — Part 2: Nanoindentation Creep and its Relationship with Uniaxial Creep as a Function of temperature. *Acta Mater.* 61: 2471-2480. DOI: <https://doi.org/10.1016/j.actamat.2013.01.020>.
- [23] Tsao, L. C., Chang, S.Y., Lee, C. I., Sun, W. H. and Huang, C. H. 2010. Effects of nano  $Al_2O_3$  Additions on Microstructure Development and Hardness of Sn3.5Ag0.5Cu Solder. *Materials and Design*. 31 (10): 4831-4835. DOI: <https://doi.org/10.1016/j.matdes.2010.04.033>.
- [24] Zhang, L., and Tu, K. N. 2014. Structure and Properties of Lead-free Solders Bearing Micro and Nano Particles. *Materials Science and Engineering R: Reports*. 82: 1-32. DOI: <https://doi.org/10.1016/j.mser.2014.06.001>.
- [25] Fahim, A., Ahmed, S., Suhling, J. C., and Lall, P. 2018. Nanoindentation Measurements of the Mechanical Properties of Individual Phases within Lead Free Solder Joints Subjected to Isothermal Aging. *ASME 2018 International Technical Conference and Exhibition on Packaging and Integration of Electronic and Photonic Microsystems, InterPACK 2018*. DOI: <https://doi.org/10.1115/IPACK2018-8408>.
- [26] Wan, Y. W. Y., Ismail, N., Safee, N. S., Ismail, A., Jalar, A., and Abu Bakar, M. 2019. Correlation of Microstructural Evolution and Hardness Properties of 99.0Sn-0.3Ag-0.7Cu (SAC0307) Lead-free Solder under Blast Wave Condition. *Soldering and Surface Mount Technology*. 31(2): 102-108. DOI: <https://doi.org/10.1108/SSMT-06-2018-0019>.
- [27] Yahaya, M. Z., Ani, F. C., Samsudin, Z., Sahin, S., Abdullah, M. Z., and Mohamad, A. A. 2016. Hardness Profiles of Sn-3.0Ag-0.5Cu-TiO<sub>2</sub> Composite Solder by Nanoindentation. *Materials Science and Engineering A*. 669: 178-186. DOI: <https://doi.org/10.1016/j.msea.2016.05.081>.
- [28] Wang, H., Hu, X., and Jiang, X. 2020. Effects of Ni Modified MWCNTs on the Microstructure Evolution and shear Strength of Sn-3.0Ag-0.5Cu Composite Solder Joints. *Materials Characterization*. 163: 110287. DOI: <https://doi.org/10.1016/j.matchar.2020.110287>.
- [29] Han, Y. D., Jing, H. Y., Nai, S. M. L., Xu, L. Y., Tan, C. M., and Wei, J. 2010. Nanomechanical Properties of a Sn-Ag-Cu Solder Reinforced with Ni-coated Carbon Nanotubes. *International Journal of Nanoscience*. 9(4): 283-287. DOI: <https://doi.org/10.1142/S0219581X10006818>.
- [30] Ismail, N., Jalar, A., Bakar, M. A., Ismail, R., Safee, N. S., Ismail, A. G., and Ibrahim, N. S. 2019. Effect of Isothermal Aging on Microhardness Properties of Sn-Ag-Cu/CNT/Cu using Nanoindentation. *Sains Malaysiana*. 48(6): 1267-1272. DOI: <https://doi.org/10.17576/jsm-2019-4806-14>.
- [31] Nai, S. M. L., Wei, J., and Gupta, M. 2006. Lead-free Solder Reinforced with Multiwalled Carbon Nanotubes. *Journal of Electronic Materials*. 35: 1518-1522. DOI: <https://doi.org/10.1007/s11664-006-0142-9>.
- [32] Liu, P., Yao, P., and Liu, J. 2008. Effect of SiC Nanoparticle additions on microstructure and microhardness of Sn-Ag-Cu Solder Alloy. *Journal of Electronic Materials*. 37: 874-879. DOI: <https://doi.org/10.1007/s11664-007-0366-3>.
- [33] Fouzder, T., Chan, Y. C., and Chan, D. K. 2014. Influence of Cerium Oxide (CeO<sub>2</sub>) Nanoparticles on the Microstructure and Hardness of Tin-silver-copper (Sn-Ag-Cu) Solders on Silver (Ag) Surface-finished Copper (Cu) Substrates. *Journal of Materials Science: Materials in Electronics*. 25: 5375-5387. DOI: <https://doi.org/10.1007/s10854-014-2316-1>.
- [34] Abdullah, I., Zulkifli, M. N., Jalar, A., and Ismail, R. 2018. Deformation Behavior Relationship between Tensile and Nanoindentation Tests of SAC305 Lead-free Solder Wire. *Soldering and Surface Mount Technology*. 30(3): 194-202. DOI: <https://doi.org/10.1108/SSMT-07-2017-0020>.
- [35] Dele-Afolabi, T. T., Azmah Hanim, M. A., Norkhairunnisa, M., and Yusoff, H. M. 2014. Physical and Mechanical Properties Enhancement of Lead-free Solders Reinforced with Carbon Nanotubes: A Critical Review. *Advances in Environmental Biology*. 8(8): 2600-2608.
- [36] Zulkifli, M. N., Jalar, A., Abdullah, S., Rahman, I. A., and Hamid, M. A. A. 2013. Strength Distribution of Au Ball Bond using Nanoindentation Approach. *Materials Science and Engineering A*. 577: 189-196. DOI: <https://doi.org/10.1016/j.msea.2013.04.059>.
- [37] Mahmudi R., Roumina R., and Raeisia B. 2004. Investigation of Stress Exponent in the Power-law Creep of Pb-Sb Alloys. *Mater. Sci. Eng. A*. 382: 15-22. DOI: <https://doi.org/10.1016/j.msea.2004.05.078>.